Acta Crystallographica Section D
Biological Crystallography
ISSN 0907-4449

Crystallization of FLINC4, an intramolecular LMO4–ldb1 complex

Janet E. Deane,[a] Megan J. Maher,[a] David B. Langley,[a] Stephen C. Graham,[a] Jane E. Visvader,[b] J. Mitchell Guss[a] and Jacqueline M. Matthews[a]*

[a]School of Molecular and Microbial Biosciences, University of Sydney, NSW 2006, Australia, and [b]Walter and Eliza Hall Institute of Medical Research, 1G Royal Parade, Parkville, VIC 3050, Australia

Correspondence e-mail: j.matthews@mmb.usyd.edu.au

Received 20 March 2003
Accepted 29 May 2003

LMO4 is the most recently discovered member of a small family of nuclear transcriptional regulators that are important for both normal development and disease processes. LMO4 is comprised primarily of two tandemly repeated LIM domains and interacts with the ubiquitous nuclear adaptor protein ldb1. This interaction is mediated *via* the LIM domains of LMO4 and the LIM-interaction domain (LID) of ldb1. An intramolecular complex, termed FLINC4, consisting of the two LIM domains from LMO4 linked to the LID domain of ldb1 *via* a flexible linker has been engineered, purified and crystallized. The trigonal crystals, which belong to space group *P*312 with unit-cell parameters a = 61.3, c = 93.2 Å, diffract to 1.3 Å resolution and contain one molecule of FLINC4 per asymmetric unit. Native and multiple-wavelength anomalous dispersion (MAD) data collected at the Zn X-ray absorption edge have been recorded to 1.3 and 1.7 Å resolution, respectively. Anomalous Patterson maps calculated with data collected at the peak wavelength show strong peaks sufficient to determine the positions of four Zn atoms per asymmetric unit.

1. Introduction

Members of the LIM-only (LMO) family are each comprised primarily of two tandemly repeated LIM domains. The term LIM is a combination of the first letter of the first three genes, namely *lin-11*, *ISL1* and *mec-3*, whose protein products contain this cysteine/histidine-rich motif. LIM domains contain two structural zinc ions and have been identified as important motifs that mediate specific protein–protein interactions. LIM domains are found in proteins with roles in diverse fundamental biological processes including cell-fate determination, trafficking, cytoskeletal organization and organ development (Bach, 2000). The presence of tandem LIM domains in LMO proteins confers the potential to engage in multiple protein–protein interactions. Indeed, LMO proteins are often found in multi-protein complexes (Wadman *et al.*, 1997; Sum *et al.*, 2002) and are thought to act as docking stations upon which multiple proteins can assemble. In particular, LMO4 has recently been shown to interact directly and simultaneously with BRCA1, CtIP and the nuclear adaptor protein LIM domain binding protein 1 (ldb1) to form a stable complex *in vivo* (Sum *et al.*, 2002). Both LMO and LIM homeodomain proteins have the ability to interact with ldb1 *via* a 39-residue region close to the C-terminus of ldb1 known as the LIM-interaction domain (LID; Jurata & Gill, 1997). Ldb1 is of particular interest as it also contains an N-terminal homodimerization domain that may allow the formation of higher order functional complexes (Jurata *et al.*, 1998).

The nuclear LMO family comprises four members, LMO1–4. Two members of this small family are known oncogenes: LMO1 and LMO2 (originally known as rhombotin and rhombotin-2, respectively) were originally discovered in patients with acute T-cell lymphoblastic leukaemia (T-ALL) and are oncogenic in mice that carry *lmo1* or *lmo2* transgenes (reviewed by Rabbitts *et al.*, 1999). LMO4 is the most recently identified member of the family. It was originally described as a breast-cancer autoantigen (Racevskis *et al.*, 1999) and has recently been shown to be overexpressed in over 50% of primary breast cancers (Visvader *et al.*, 2001). Both LMO4 and ldb1 appear to act as negative regulators of breast epithelial differentiation (Visvader *et al.*, 2001). Furthermore, displacement of LMO4 as the binding partner of ldb1 by overexpression of either LMO1 or LMO2 has been proposed as a mechanism for LMO-induced T-ALL (Rabbitts, 1998).

Previously, we have described the design and production of a fusion protein in which ldb1-LID and LIM1 of LMO4 were linked to form an intramolecular complex (Deane *et al.*, 2001). The structure of this complex was solved using multidimensional NMR spectroscopy (Deane *et al.*, 2003). Analysis of this structure suggested that the second LIM domain of LMO4 might also be important for the inter-

action with ldb1-LID. This led to the design of an extended fusion construct that includes both LIM domains of LMO4. This 20 kDa protein, termed FLINC4 (an abbreviation of 'fusion of ldb1-LID and the N- and C-terminal LIM domains of LMO4'), consists of residues 16–152 of LMO4 (DDBJ/EMBL/GenBank accession No. XM_030627), including the two LIM domains, and residues 300–339 of ldb1 (encompassing the LID; DDBJ/EMBL/GenBank accession No. NM_003893). The LMO4 and ldb1 portions of FLINC4 are fused *via* a flexible linker comprised of 11 glycine and serine residues. Here, we report on the production, crystallization and preliminary crystallographic analysis of FLINC4.

2. Experimental procedures

2.1. Production and purification

The production of the coding sequences for LMO4 and ldb1 and the methodology for production of the fusion protein FLIN4 have been described previously (Deane *et al.*, 2001). The insert encoding FLINC4 was produced using overlap extension PCR to encode the following protein sequence: GSLSWKRCAGCGGKIADRFLLYAMD-SYWHSRCLKCS**S**CQAQLGDIGTS**S**YT-KSGMILCRNDYIRLFGNSGACSACGQ-SIPASELVMRAQGNVYHLKCFTCSTC-RNRLVPGDRFHYINGSLFCEHDRPTA-LINGHLN*SGGSGGSGGSGG*DVMVVG-EPTLMGGEFGDEDERLITRLENTQFD-AANGIDDE, where the italicized residues form an artificial linker and Cys-to-Ser mutations are indicated in bold. This insert was subcloned into the pGEX-2T vector using *Bam*H1 and *Eco*R1 restriction sites and then sequenced for confirmation. FLINC4 was overexpressed and purified as previously described for FLIN4 (Deane *et al.*, 2001) and the purified protein was concentrated in Centricon YM-3 centrifugal filtration devices (Millipore) to a concentration of 13 mg ml^{-1}. Samples of concentrated FLINC4 (1.0 ml) were dialysed against 20 m*M* Tris pH 8.0, 1 m*M* Tris (2-carboxyethyl)phosphine hydrochloride (TCEP) and 150 m*M* NaCl before crystallization.

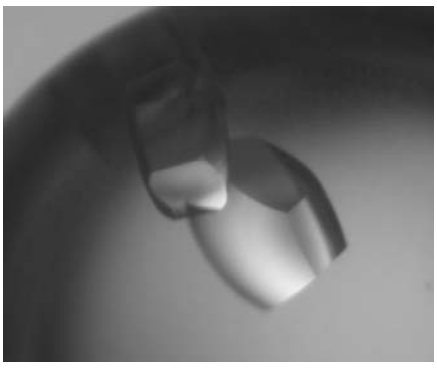

Figure 1
Trigonal crystals of FLINC4. Typical dimensions are 800 × 500 × 400 µm.

2.2. Crystallization

Preliminary crystallization conditions were found using factorial screens (Jancarik & Kim, 1991) by the hanging-drop vapour-diffusion method. Each of the solutions from Hampton Crystal Screens 1 and 2 (Hampton Research, CA, USA) (1.5 µl) was mixed with a solution of FLINC4 (1.5 µl) at room temperature (293 K). Crystals were observed after 4 d under five different conditions (Hampton Screen 1 condition 18 and Hampton Screen 2 conditions 20, 23, 42 and 45).

Initial refinement from Hampton Screen 2 condition 23 (1.6 *M* ammonium sulfate, 0.1 *M* MES pH 6.5, 10% dioxane) yielded the best crystals. Crystals that diffracted to 1.3 Å resolution grew under conditions where hanging drops were prepared by mixing 2.0 µl of protein solution with an equal volume of reservoir solution (1.0 *M* ammonium sulfate, 0.1 *M* MES pH 6.7) and were equilibrated against 0.5 ml of reservoir solution at 293 K. Crystals appeared overnight (Fig. 1).

2.3. Diffraction data and crystallographic calculations

Crystals were cryoprotected by successive soaking in mother liquor containing increasing quantities of glycerol [the final concentration of glycerol was 25%(*v*/*v*)] and flash-frozen in a cold nitrogen-gas stream for data collection. The Zn atoms present in FLINC4 were used as anomalous scatterers for structure determination using the multiple-wavelength anomalous dispersion (MAD) method. Data sets were collected at 100 K from a single frozen crystal of FLINC4 on beamline 1-5 of the Stanford Synchrotron Radiation Laboratory (SSRL) using an ADSC Q4 CCD detector. A broad X-ray excitation scan of the crystal gave an intense absorption edge at 9665 eV, characteristic of the presence of zinc. Data were collected at three wavelengths near the zinc absorption edge: λ_1, 1.282 Å, 9669 eV (the f'' peak); λ_2, 1.170 Å, 10600 eV (a high-energy remote from the absorption edge); λ_3, 1.283 Å, 9665 eV (the inflection point). Native diffraction data were collected at 100 K on beamline 7-1 at SSRL using a MAR 345 image-plate detector (Fig. 2). The data were recorded in two passes to prevent overloading of the low-angle data. The first pass to record the high-resolution data (to 1.3 Å) had 60 s exposure times and a crystal-to-detector distance of 130 mm. The second pass for the low-resolution data (2.4 Å) had 10 s exposures and a crystal-to-detector distance of 350 mm. All data were integrated and scaled with *DENZO* and *SCALEPACK* from the *HKL* program suite (Otwinowski & Minor, 1991). Anomalous and dispersive difference Patterson functions were calculated from the MAD data using the *CNS* program suite (Brünger *et al.*, 1998). Heavy-atom positions were determined using automated Patterson methods as implemented in *SOLVE* (Terwilliger & Berendzen, 1999).

3. Results and discussion

Large barrel-like crystals of FLINC4 grew overnight using 1.0 *M* ammonium sulfate as the precipitant. The symmetry and lack of systematic absences in the diffraction data show that the crystals are trigonal, space group *P*312, with unit-cell parameters a = 61.3, c = 93.2 Å. The value of the Matthews coefficient is 2.50 Å^3 Da^{-1} for one molecule per asymmetric unit (188 residues, 20.0 kDa), corresponding to a solvent content of 50.0% (Matthews, 1968).

Very high resolution (1.3 Å) diffraction data were collected using synchrotron radiation at SSRL (Fig. 2). In addition, MAD data to 1.7 Å were collected from a single FLINC4 crystal at three wavelengths about the zinc X-ray absorption edge. Analysis of anomalous and dispersive difference Patterson maps calculated to the resolution limit of the data clearly showed the presence of ordered zinc sites (Fig. 3).

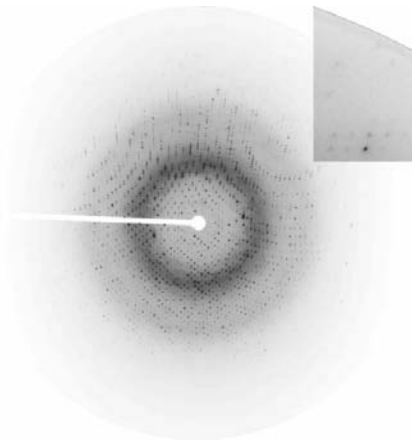

Figure 2
Diffraction image recorded from a crystal of FLINC4. The inset shows data at the limit of diffraction (1.3 Å).

Table 1
Data-collection statistics.

Values for the highest resolution shell are given in parentheses.

	MAD			
	λ_1	λ_2	λ_3	Native
Wavelength (Å)	1.282	1.170	1.283	1.08
Resolution limit (Å)	1.7 (1.76–1.70)	1.7 (1.76–1.70)	1.7 (1.76–1.70)	1.3 (1.35–1.30)
Mosaicity (°)	0.38	0.38	0.38	0.36
Completeness (%)	99.7 (99.4)	99.6 (99.2)	99.7 (99.5)	91.3 (79.2)
Unique reflections	22274	22282	22284	45441
Redundancy	5.1 (4.9)	5.2 (4.8)	5.1 (4.9)	2.6 (2.0)
$R_{\rm merge}$†	0.061 (0.464)	0.051 (0.290)	0.054 (0.489)	0.040 (0.291)
$I/\sigma(I)$	20.2 (3.2)	19.2 (3.7)	18.7 (3.0)	18.0 (2.4)
Data with $I > 3\sigma(I)$ (%)	85.6 (48.0)	85.1 (46.1)	89.6 (64.7)	83.5 (41.2)

† $R_{\rm merge} = \sum(|I - \langle I\rangle|)/\sum(I)$, where I is the intensity of an individual measurement of each reflection and $\langle I\rangle$ is the mean intensity of that reflection.

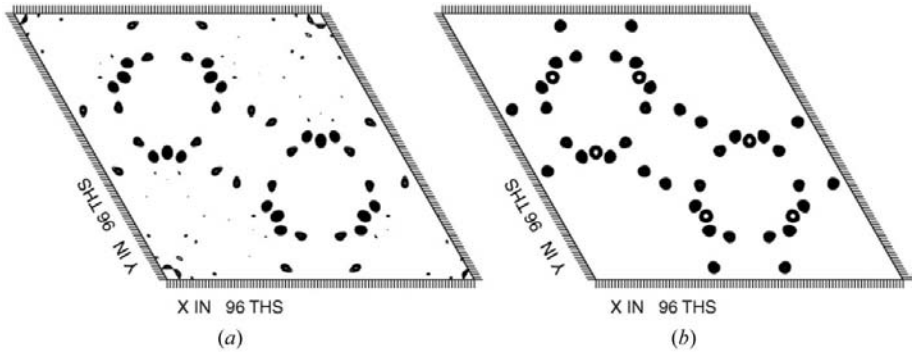

Figure 3
Anomalous difference Patterson maps of FLINC4. (*a*) Calculated with data collected at 1.282 Å (Table 1) to 2.0 Å resolution; (*b*) calculated from predicted zinc sites. The unit cell of the Harker section (z = 0) is shown. Maps are drawn with a minimum contour level of 2σ, with 0.5σ increments.

The positions of four Zn atoms per asymmetric unit were determined and refined with an overall figure of merit of 0.75 for all reflections in the resolution range 20–1.7 Å. Interpretation of the resulting electron-density maps is in progress.

This research was supported by the following grants from the Australian Research Council: Project Grant A10009131, a Postdoctoral Fellowship to MJM and a Research Fellowship to JMM. JED and SCG are supported by Australian Postgraduate Awards. Access to the facilities of the Stanford Synchrotron Radiation Laboratory was made possible by a travel grant from the Access to Major National Facilities Programme administered by the Australian Nuclear Science and Technology Organization. Portions of this research were carried out at the Stanford Synchrotron Radiation Laboratory, a national user facility operated by Stanford University on behalf of the US Department of Energy, Office of Basic Energy Sciences. The SSRL Structural Molecular Biology Program is supported by the Department of Energy, Office of Biological and Environmental Research, by the National Institutes of Health, National Center for Research Resources, Biomedical Technology Program and the National Institute of General Medical Sciences.

References

Bach, I. (2000). *Mech. Dev.* **91**, 5–17.
Brünger, A. T., Adams, P. D., Clore, G. M., DeLano, W. L., Gros, P., Grosse-Kunstleve, R. W., Jiang, J. S., Kuszewski, J., Nilges, M., Pannu, N. S., Read, R. J., Rice, L. M., Simonson, T. & Warren, G. L. (1998). *Acta Cryst.* D**54**, 905–921.
Deane, J. E., Mackay, J. P., Kwan, A. H. Y., Sum, E., Visvader, J. E. & Matthews, J. M. (2003). *EMBO J.* **22**, 2224–2233.
Deane, J. E., Sum, E., Mackay, J. P., Lindeman, G. J., Visvader, J. E. & Matthews, J. M. (2001). *Protein Eng.* **14**, 493–499.
Jancarik, J. & Kim, S.-H. (1991). *J. Appl. Cryst.* **24**, 409–411.
Jurata, L. W. & Gill, G. N. (1997). *Mol. Cell. Biol.* **17**, 5688–5698.
Jurata, L. W., Pfaff, S. L. & Gill, G. N. (1998). *J. Biol. Chem.* **273**, 3152–3157.
Matthews, B. W. (1968). *J. Mol. Biol.* **33**, 491–497.
Otwinowski, Z. & Minor, W. (1991). *Methods Enzymol.* **276**, 307–326.
Rabbitts, T. H. (1998). *Genes Dev.* **12**, 2651–2657.
Rabbitts, T. H., Bucher, K., Chung, G., Grutz, G., Warren, A. & Yamada, Y. (1999). *Cancer Res.* **59**, *Suppl.* 7, 1794s–1798s.
Racevskis, J., Dill, A., Sparano, J. A. & Ruan, H. (1999). *Biochim. Biophys. Acta*, **1445**, 148–153.
Sum, E. Y., Peng, B., Yu, X., Chen, J., Byrne, J., Lindeman, G. J. & Visvader, J. E. (2002). *J. Biol. Chem.* **277**, 7849–7856.
Terwilliger, T. C. & Berendzen, J. (1999). *Acta Cryst.* D**55**, 501–505.
Visvader, J. E., Venter, D., Hahm, K., Santamaria, M., Sum, E. Y., O'Reilly, L., White, D., Williams, R., Armes, J. & Lindeman, G. J. (2001). *Proc. Natl Acad. Sci. USA*, **98**, 14452–14457.
Wadman, I. A., Osada, H., Grutz, G. G., Agulnick, A. D., Westphal, H., Forster, A. & Rabbitts, T. H. (1997). *EMBO J.* **16**, 3145–3157.